INFLUENCE OF THE URBAN SOLAR CAR VELOCITY ON THE DRAG COEFFICIENT

[1]P. MIERZEJEWSKA, [2]A. CIESLINSKI, [3]J. SZCZOTARSKI, [4]T. BURZYNSKI, [5]T. PAŁCZYNSKI

Lodz University of Technology, Institute of Turbomachinery, Lodz, Poland
E-mail: [1]221885@edu.p.lodz.pl, [2]a.cieslinski0@gmail.com, [3]197221@edu.p.lodz.pl, [4]226697@edu.p.lodz.pl, [5]tomasz.palczynski@p.lodz.pl

Abstract - The purpose of theresearch is to analyse the aerodynamic properties of solar car Eagle Two for the sake of solar car competitions. The article focuses on the determination of drag force and drag coefficient as a function of velocity. The research was performed in ANSYS CFX software. The numerical simulations were performed for five chosen test speeds – 10, 40, 70, 100 and 130 km/h. The study provides analysis of static pressure distribution, velocity profile, velocity streamlines and turbulence intensity plots. The authors analyse the approximation method based on the obtained results of drag coefficients.

Index terms - Boundary layer separation, CFD, drag coefficient, drag force, numerical simulation, vehicle aerodynamics

I. INTRODUCTION

The purpose of the Lodz Solar Team project is participation in the internationalsolar car races – Bridgestone World Solar Challenge and Ilumen European Solar Challenge. For the sake of the competitions the students of Lodz University of Technology constructed and built a 5-person urban solar vehicle Eagle Two, which is a second prototype after Eagle One. All solar car competitions in the urban category base not only on the time of race completion but primarily on the efficiency of the solar car with reference to the distance covered and number of passengers on board. Hence, in order to prepare satisfactory strategy plan it is of particular significance to know the energy consumption of the vehicle at different velocities. Therefore, the research was aimed at determining the dependence of the velocity on the drag coefficient of a solar car. The formula for the results of Ilumen European Solar Challenge 2018 is as follows

$$\frac{\text{battery capacity} \cdot \text{no. of charging}}{\text{laps}^{1.8} \cdot (0.5 \cdot \text{passengers} + 0.5)}. \qquad (1)$$

The car with the lowest results takes the highest place. As far as energy consumption is concerned it has to be considered that the motor thrust force has to overcome two drag components – aerodynamic drag force and rolling friction force [1]

$$F_t = F_d + F_f, \qquad (2)$$

where: F_t – motor thrust force, F_d – aerodynamic drag force, F_f – rolling friction force.
It is known that aerodynamic drag force is dependent on the fluid flow but the frictional force is dependent on it as well. This is due to the fact that the formula for rolling friction force is dependent on the reactive normal force, hence on the lift force

$$F_f = f \cdot F_n = f \cdot (F_g - F_l), \qquad (3)$$

where: F_f – rolling friction force, F_n – reactive normal force, F_g – gravitational force, F_l – aerodynamic lift force.
However, due to the fact that frictional force is dependent on the rolling resistance coefficient of the tyres which in our case is$f \in (0.0023\,;0.00268)$, the key factor in the drag formula is the aerodynamic drag force (approximately 85% of the total drag).
As far as aerodynamics is concerned, it is known that during a viscous flow past a body (or body moving in a viscous fluid) there has to be considered an aerodynamic force acting on that body. On each element of that body there acts a normal force proportional to the static pressure and tangential force proportional to tangential stress [2]. Hence, the aerodynamic force (due to friction (viscosity) and surface pressure distribution) is dependent on Reynolds number and shape and roughness of the body [3,4]. The total aerodynamic force can be resolved into two components – drag force (in the direction of relative motion) and lift force (in the direction perpendicular to the motion direction).

The action of friction and pressure drag on an object is presented in the Figure 1.

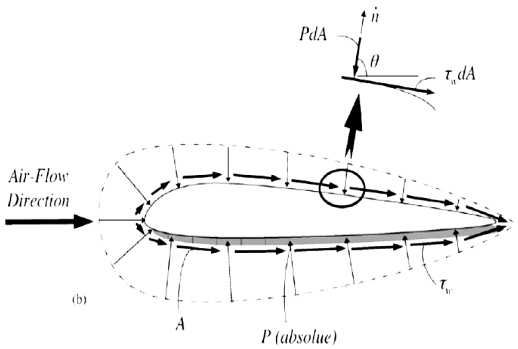


Figure 1. Aerodynamic force acting on a body [3]

The formula for the total drag (due to pressure distribution and friction) is, hence, as follows [3]

$$\vec{F}_{drag} = \int_A (\tau\vec{t} - P\vec{n})dA. \qquad (4)$$

where: τ – tangential stress, $\vec{t}$ – unit tangential vector, τ – pressure, $\vec{n}$ – unit normal vector, A – area.
However, in case of the research Reynolds number is significantly higher than 1, thus the drag force is mainly due to the pressure distribution on the body (the difference between pressure at front and rear), which is due to the changing velocity around the body. With flow velocity deceleration the static pressure increases, and with increasing flow velocity it decreases. For $Re < 1$, on the other hand, the drag force is caused by the fact that moving body propels adjacent fluid layers. The layers directly adhering to the body move with velocity of that body, whereas further layers move with smaller velocity, what causes friction.

The general formula for drag force can also be expressed as a function ofdifferent factors – velocity of the relative motion, object characteristic area (frontal area in this case), fluid density and drag coefficient [3-7]

$$F_{drag} = c_d \rho A \frac{v^2}{2}, \qquad (5)$$

where: c_d – drag coefficient, A –object characteristic area, v –object velocity.
Drag coefficient is the parameter dependent on the shape and roughness of the body, hence it determines how well streamlined the body is. The Figure 2 presents drag coefficient as a function of Reynolds number for different 3-dimensional shapes.

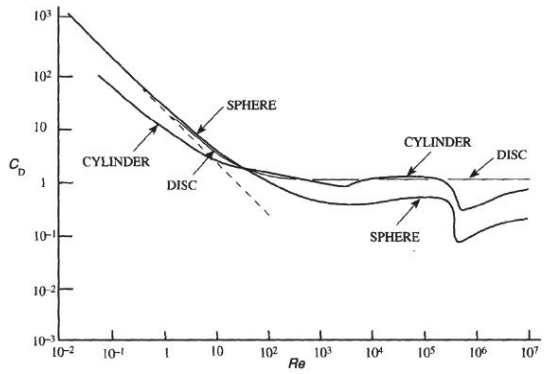


Figure 2. Drag coefficient for different objects [8]

As it is visible the c_d coefficient is higher for smaller Re (hence smaller velocities) and it decreases with increasing velocity (to finally reach the point of drag crisis in case of sphere and cylinder). The function has a similar course for all presented shapes.

II. RESEARCHED OBJECT

The article bases on the aerodynamic research of a solar urban vehicle Eagle Two. The design of the vehicle was restricted by the regulations of the competitions – i.e. maximum photovoltaic panels area, maximum vehicle dimensions or the angles of position of the drivers and passengers in the car, which determined the minimum height of the vehicle. The dimensions of Eagle Two are 4.95 m × 1.60 m × 1.30 m (length × width × height) and its weight is approximately 380 kg (carbon fibre body). The frontal area of the vehicle is 1.61 m^2. The 3-dimensional model of the car is presented in the Figure 3. The model prepared for the CFD simulations is a simplified version of the vehicle construction. The geometry includes car body and wheels, however more complex elements of the construction such as suspension, gaps and other irregularities were neglected due to the limitations of the software ANSYS CFX

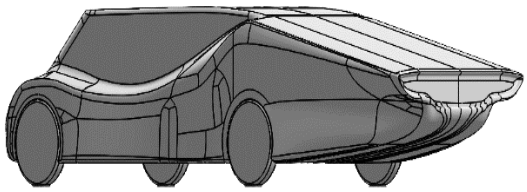


Figure 3. Eagle Two model

The idea of the rear diffusor design was to avoid boundary layer separation and distribute flow evenly on the rear part of the car, so that the pressure could be recovered and drag was lowered.

III. CFD model

For the purpose of the research ANSYS CFX software was applied and the aerodynamic tunnel of dimensions 65 × 10 × 12 m (length × width × height) was created. The dimensions of the tunnel were calculated in order to avoid blockage effect and observe complex phenomenon taking place behind the car. In order to create regions of finer mesh the tunnel was divided into different volumes – cuboid containing the vehicle and directly behind where the turbulences occur. The overview on the geometry of the aerodynamic tunnel is presented in the Figure 4.

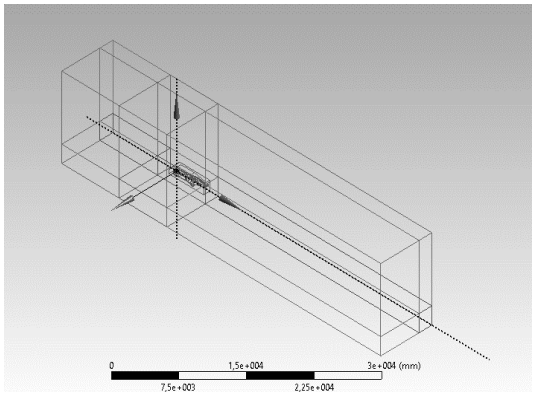


Figure 4. CFD wind tunnel

The tunnel was meshed using patch conforming method with tetrahedral elements. The body sizing on key volumes and surface sizing with inflation layers on car body surfaces was applied. The mesh is presented in the Figure 5.

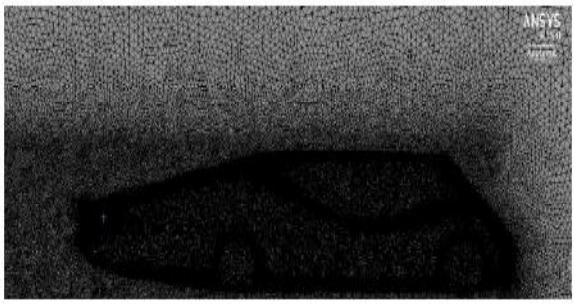


Fig. 5. Mesh around the vehicle

As far as setup is concerned, the following conditions were applied:

- Domain: Air Ideal Gas (Continuous Fluid),
- Heat transfer option: Isothermal,
- Fluid temperature: 25 ˚C,
- Flow model: Stationary
- Turbulence model: Shear Stress Transport.

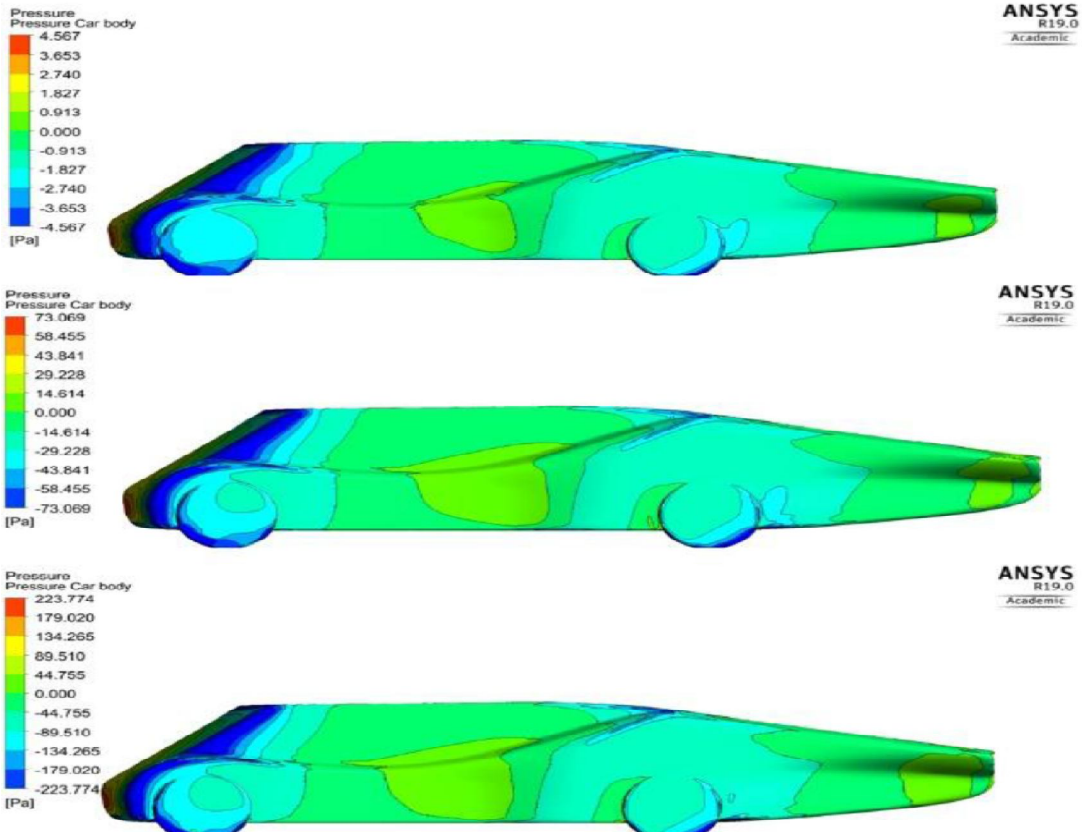
The concept of the research is based on the simulation of the stationary vehicle in a tunnel with flowing fluid, hence the following conditions were applied in order to simulate real-life conditions:

- Inlet normal speed: 10, 40, 70, 100, 130 km/h (considered vehicle speed),
- Outlet relative pressure: 0 Pa (reference pressure: 1 atm),
- Wheels: No slip wall, Rotating Wall (corresponding to the velocity of vehicle),
- Road: No slip wall, wall velocity (considered vehicle speed),
- Car body: Smooth Wall, No Slip Wall,
- Symmetry condition (half of the geometry was simulated due to the hardware limitations).

IV. SIMULATION RESULTS

During the research there were performed simulations for five chosen velocities – 10, 40, 70, 100 and 130 km/h. Figure 6 presents static pressure distribution at the side and bottom of the model for each velocity. As it is visible in the plots the pressure distribution on car body is very similar in all cases.

The regions of high and low pressure are placed in the same places on the body. As far as pressure values are concerned the maximum static pressure changes from approximately $4.6\,Pa$ (at $10km/h = 2.78\,m/s$) to $771.8Pa$ ($130\ km/h = 36.11m/s$)– the static pressure increases as velocity squared. Changes of pressure contours in the direction different than perpendicular to the motion direction (at the bottom view)suggest that there are transverse pressure gradients which result in mixing and turbulence creation and hence decreased pressure recovery.



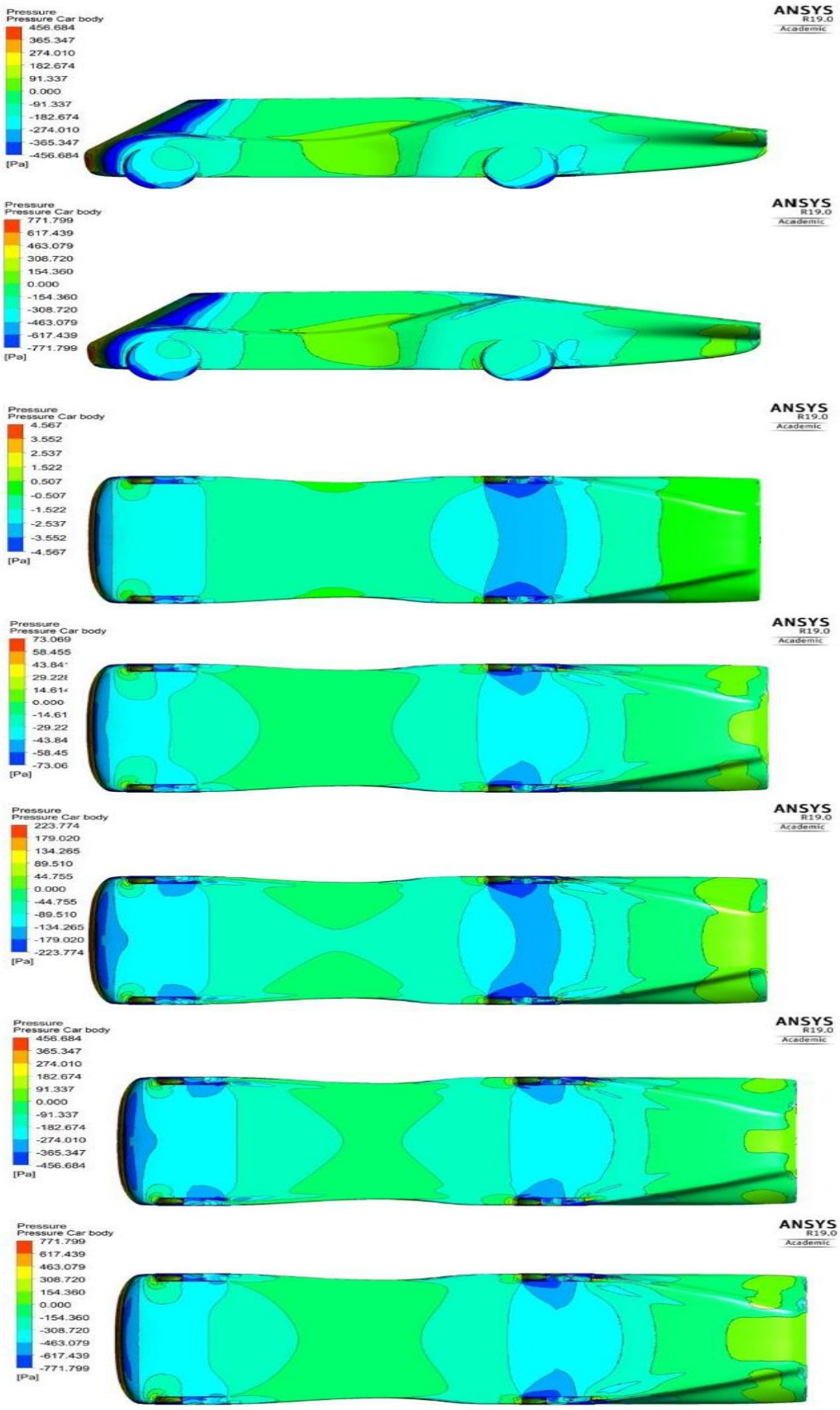


Figure 6. Static pressure distributionat vehicle side and bottom(10 km/h, 40 km/h, 70 km/h,100km/h, 130 km/h top down)

It is known the predominant part of the drag force at considered velocities (Reynolds numbers) is due to static pressure distribution and particular pressure recovery at the rear of the vehicle. The results of the aerodynamic drag force corresponding to the considered velocities are presented in the Table 1.

Table 1. Aerodynamic drag force

Velocity [km/h]	10	40	70	100	130
Velocity [m/s]	2.78	11.11	19.44	27.78	36.11
Drag Force [N]	1.5	18.1	51.9	102.3	164.4

Figure 7 presents the dependence of the velocity on the aerodynamic drag force, frictional force and total drag force for the researched model. As it is visible in the plot for velocities above approximately 10 km/h=2.78 m/s aerodynamic drag has prevailing impact on the total drag.

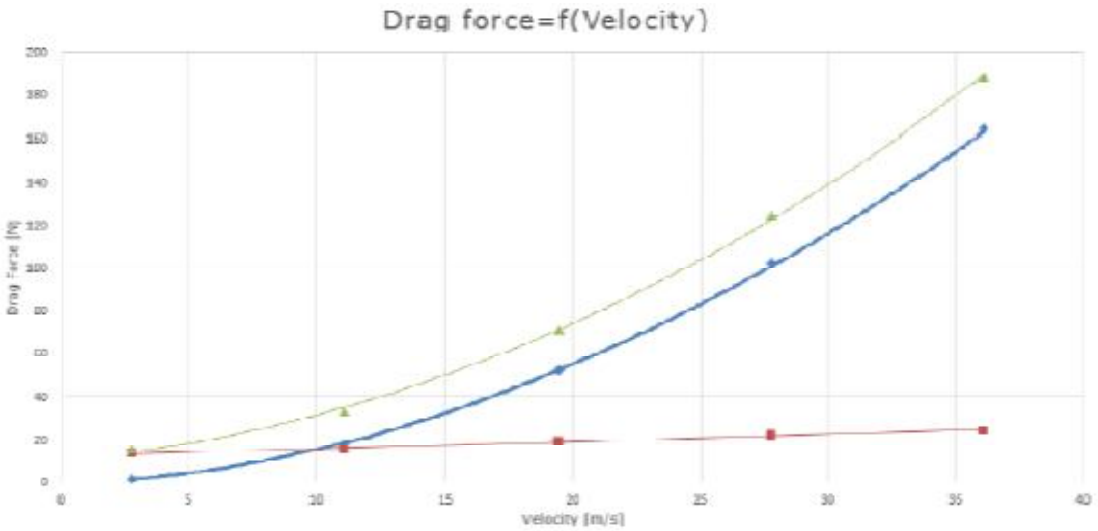
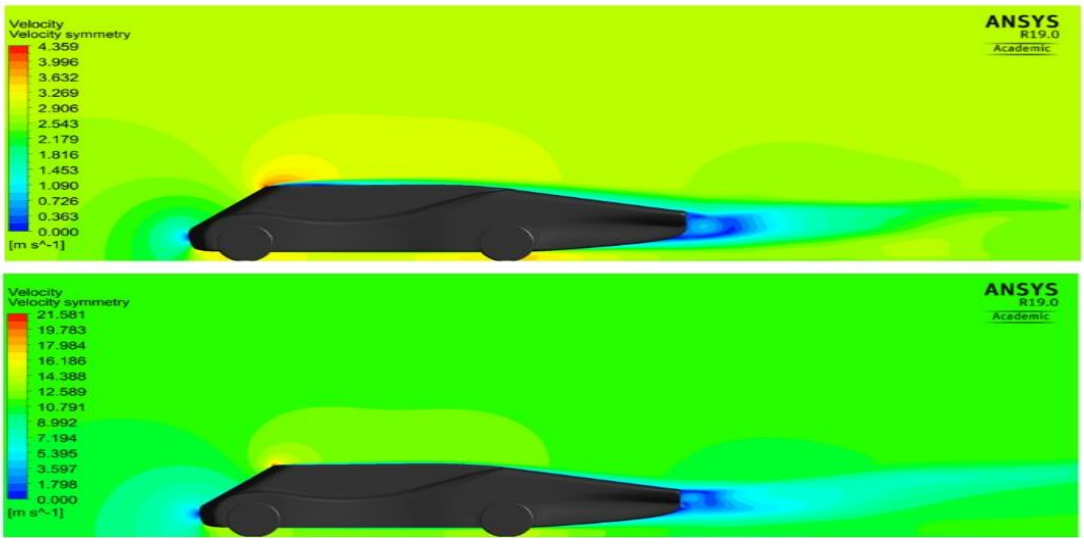
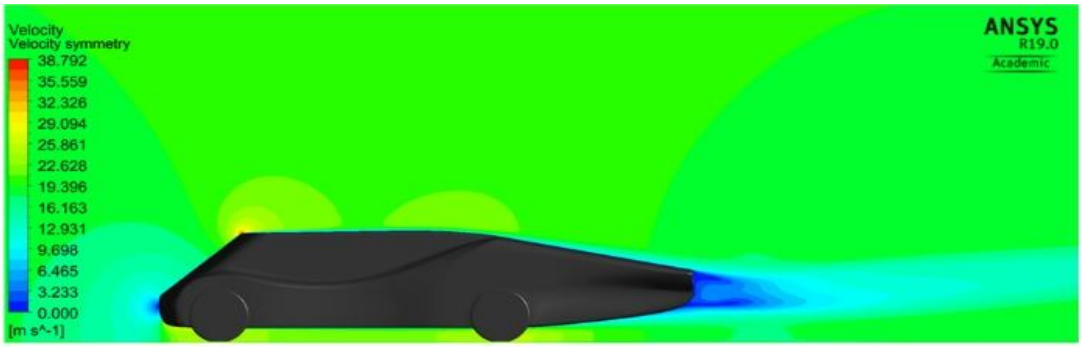
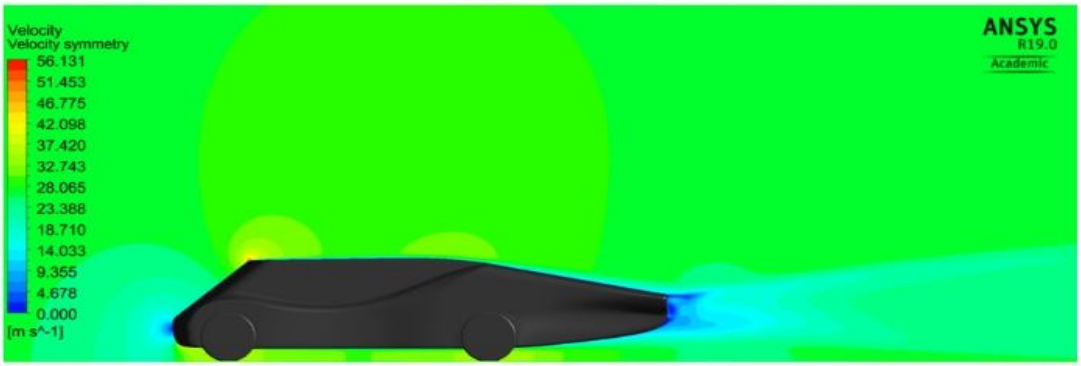


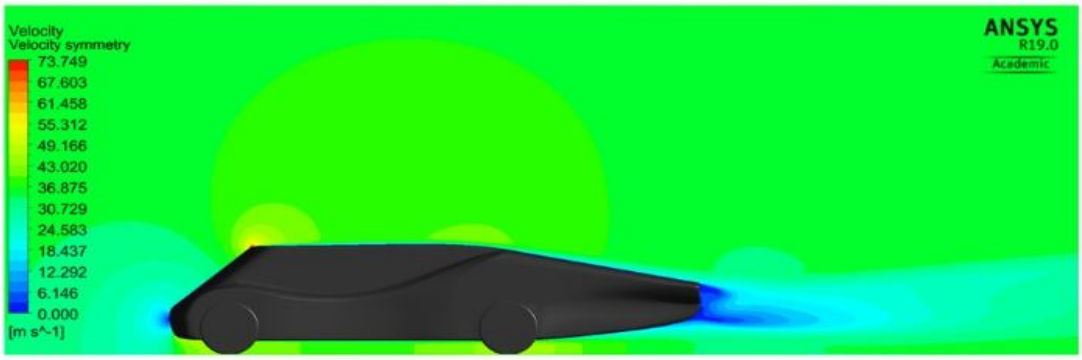
Figure 7. Total drag force (green), aerodynamic drag (blue), frictional force (red)

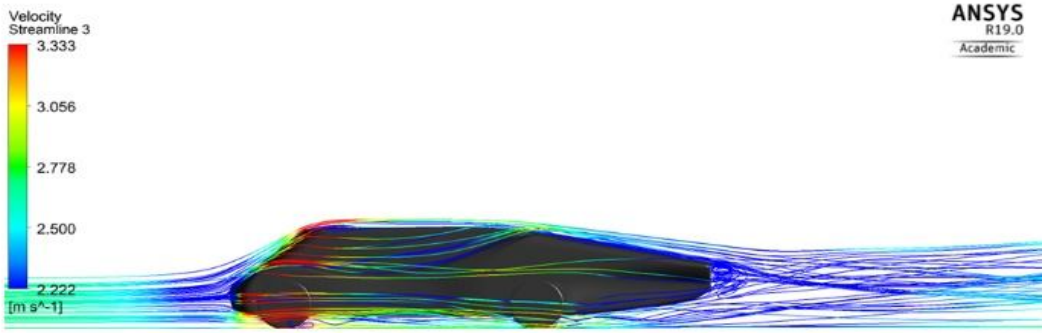
In the Figure 8 there are presented velocity contours and streamlines for all five cases respectively. It is visible that in case of the lowest velocity ($10\,km/h = 2.78\,m/s$) the separation bubble at the front (top of the windscreen) of the vehicle is the biggest. With increasing velocity the separation bubble size decreases (the smallest was noticed for $130\,km/h$). There is also observed a region of increased velocity below the car model in the first case. Such phenomena results in decreased pressure in that area, hence worse pressure recover at the rear. It was also noticed that the separation point occurs earlier for the lower velocities. It is clearly visible for the lowest velocity. The streamline plots also present that the wake zone is bigger for smaller velocities. In case of higher velocities the flow sticks better to the car body hence boundary layer separation occurs later and the turbulent wake is smaller (noticeable particularly for the bottom streamlines).

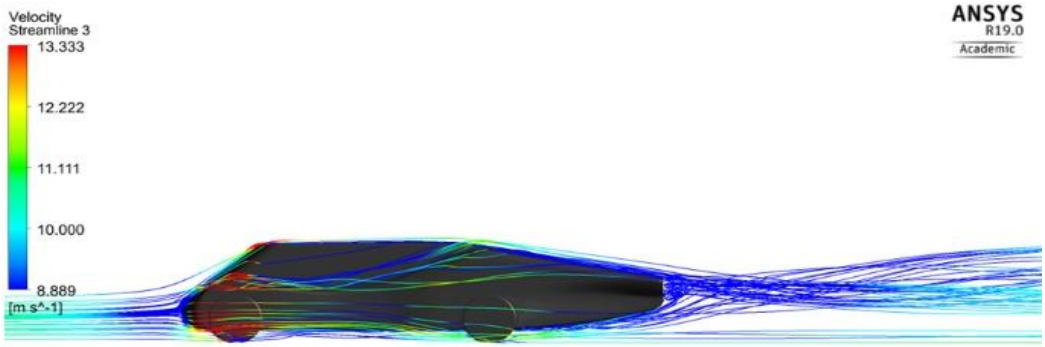



Velocity
Velocity symmetry
38.792
35.559
32.326
29.094
25.861
22.628
19.396
16.163
12.931
9.698
6.465
3.233
0.000
[m s^-1]
ANSYS
R19.0
Academic


Velocity
Velocity symmetry
56.131
51.453
46.775
42.098
37.420
32.743
28.065
23.388
18.710
14.033
9.355
4.678
0.000
[m s^-1]
ANSYS
R19.0
Academic


Velocity
Velocity symmetry
73.749
67.603
61.458
55.312
49.166
43.020
36.875
30.729
24.583
18.437
12.292
6.146
0.000
[m s^-1]
ANSYS
R19.0
Academic


Velocity
Streamline 3
3.333
3.056
2.778
2.500
2.222
[m s^-1]
ANSYS
R19.0
Academic


Velocity
Streamline 3
13.333
12.222
11.111
10.000
8.889
[m s^-1]
ANSYS
R19.0
Academic

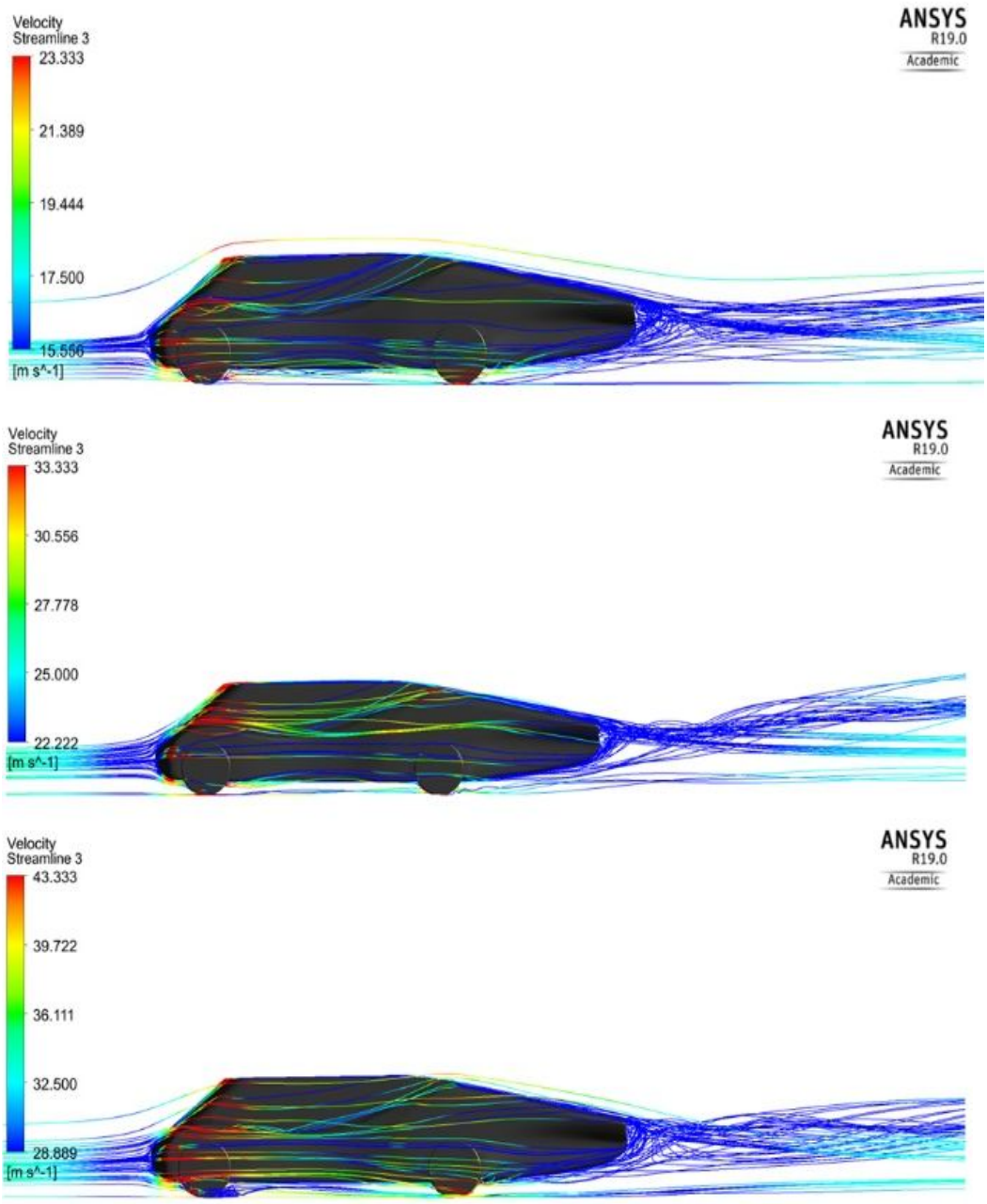


Figure 8. Velocity contour and streamlines (10 km/h, 40 km/h, 70 km/h, 100km/h, 130 km/h top down)

V. DRAG COEFFICIENT ESTIMATION

Table 2 presents drag coefficient results for researched velocities. As it was noticeable in the Figures 7-8 the highest value was obtained for the lowest velocity of $10\,km/h\,(2{,}78\,m/s)$. The value of drag coefficient decreases with velocity.

Table 2. Drag coefficient

Velocity [km/h]	10	40	70	100	130
Velocity [m/s]	2,78	11,11	19,44	27,78	36,11
Drag coefficient [-]	0,199	0,153	0,143	0,138	0,132

The authors reviewed the literature seeking approximation proposals [9-12]. There were found four examples ofdrag coefficient testing against velocity for vehicles and the results are presented in the Figure9.

The authors tested different approximation types on the gathered data and as it turned out power approximation fitted most satisfyingly in all four cases. Due to the fact that drag coefficient is a complex parameter dependent on various variables such as Reynolds number, surface roughness, shape of the object the approximation functions differ for each presented case.

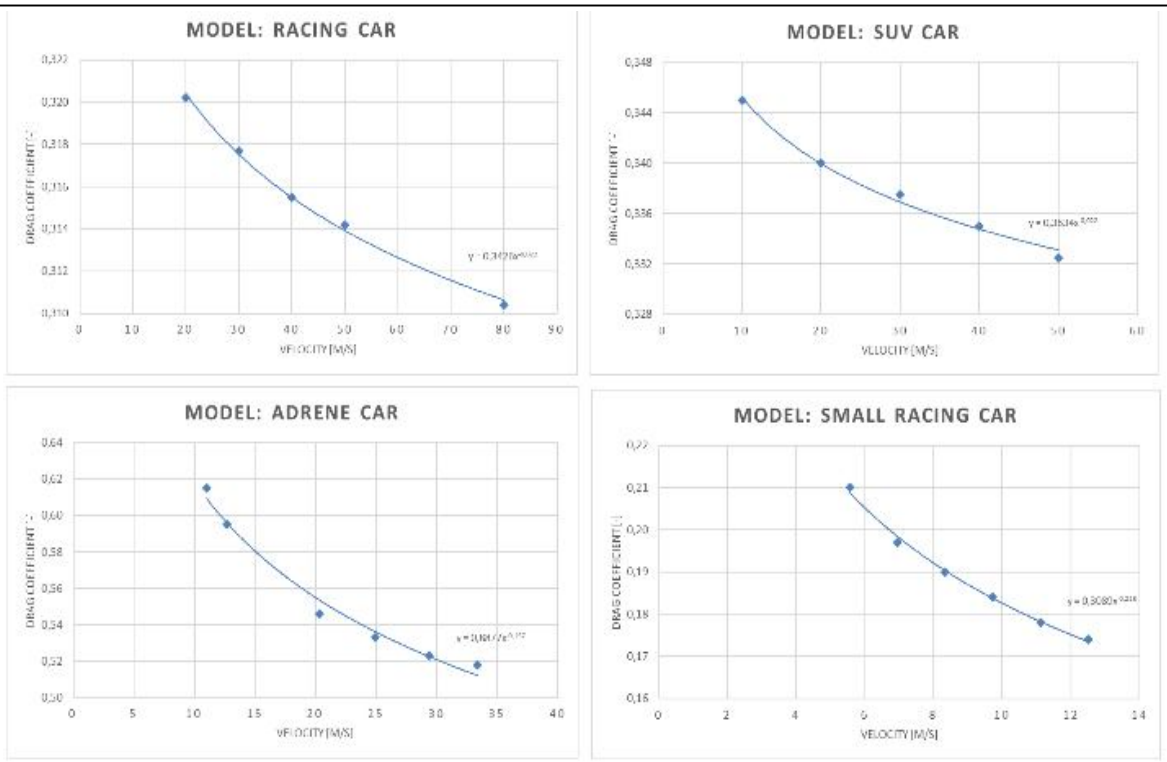


Figure9. Drag coefficient as a function of velocity for different vehicles (racing car – top left, SUV car – top right, Adrene car – bottom left, small racing car – bottom right) [9-12]

For the above presented literature results (Figure 9) there is a quite good method of their approximation using power function. The coefficient of determination R^2 confirms the rightness of the approximation – 1.00 for the racing car, 0.99 for the SUV car, 1.00 for the Adrene car and 0.99 for the small racing car. Hence, the authors propose a power approximation of the function of drag coefficient versus velocity for Eagle Two (Figure 10). The coefficient of determination in this case is equal 0.99.

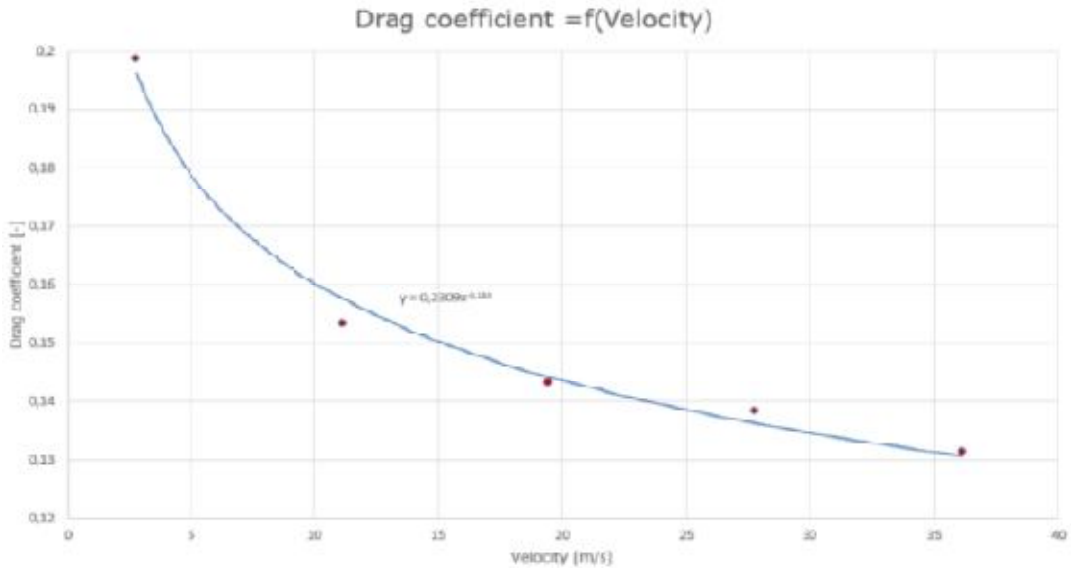


Figure 10. Drag coefficient as a function of velocity for Eagle Two

As it is visible in the Figure 10 the value of drag coefficient decreases with velocity. This is due to the fact that for smaller velocities the separation of the boundary layer occurs earlier. In case of turbulent boundary layer the more energetic particles inside it transfer some of its energy to the elements directly adjacent to the solid surface. Inside the layer there occurs and exchange of more and less energetic particles. Such phenomena slows down the kinetic energy loss due to the impeding forces, and hence the separation.

Therefore for higher velocities the energy transferred inside the boundary layer is higher and thus separation occurs later.

CONCLUSIONS

In conclusions, the research included aerodynamic simulations of a solar car Eagle Two. There were presented plots visualising the flow around the car body at different speeds. It is clearly visible that the flow character changes with velocity. The smaller the velocity the earlier the boundary layer separation occurs, the higher the wake zone ant turbulences and hence, the higher the drag coefficient. It was observed that the drop of the drag coefficient in the first part of the plot is more rapid than in later parts. That is due to the fact that small increase in the velocity stalls the separation of the boundary layer significantly causing smaller turbulence wake and hence decreasing the drag coefficient essentially. Reaching the velocity of 10km/h (2.78 m/s) the function slows down and the decrease becomes less sharp (such behaviour was also observed in the cited results).

The lowest value of the drag coefficient was obtained for 130 km/h(36.11 m/s) and is equal to 0.132. The authors also proposed a power approximation of the drag coefficient function, based on the researched literature, which allows evaluation of the values of drag coefficient for different, not tested velocities, and hence strategy preparation is possible. However, even though drag coefficient is significantly higher for low velocities and the flow is less structured and sticking to the body the aerodynamic drag force increases with velocity.

This is due to the fact that the drag force is dependent on the square of velocity. The smaller the velocity the smaller the static pressure at the front of the vehicle due to isentropic standstill of the fluid. Small static pressure at the front generates small pressure loses to recover at the rear and hence, even though the drag coefficient is larger the drag force is lower.

REFERENCES

[1] Srinivas VL., “Shape Optimization of a Car Body for Drag Reduction and to Increase Downforce”, J. N. T. University Anantapur, April 2016

[2] Kosma Z., ”Podstawy mechaniki płynów”, Politechnika Radomska, 2005

[3] White FM., “Fluid mechanics”, Boston, McGraw-Hill Book Company, 2003

[4] Vennard JK.,“Elementary fluid mechanics”, Read Books Ltd, 2013

[5] Osborne J., “The Variation of Profile Drag with Mach Number Up to the Critical Value: A Comparison of Recent Predictions with Early Flight and Wind-tunnel Measurements and a Comment on an Earlier Prediction”, National Physical Laboratory, June 1966.

[6] Munson B. R., Young D. F., and Okiishi T. H., “Fundamentals of Fluid Mechanics”, Wiley, New York, 1990.

[7] Sakamoto H., Haniu H., “A study on vortex shedding from spheres in a uniform flow”, Journal of Fluids Engineering, pp. 386-392, December 1990

[8] Caballero R., Vega A., Berbey A., Armanda M., “Six degree of freedom underwater vehicle for culvert inspection”, CLAWAR 2014 – Proceedings of the Seventeenth International Conference on Climbing and Walking Robots and the Support Technologies for Mobile Machines, Poznan, July 2014

[9] Hassan SR, Islam T, Ali M, Islam MQ.,“Numerical study on aerodynamic drag reduction of racing cars”, Procedia Engineering, pp. 308-313, January 2014

[10] Shankar G., Devaradjane G., Sunil S., “Investigation on Aerodynamic Behaviour of a SUV Car Model with Vortex Generators at Different Yaw Conditions”, Journal of Applied Fluid Mechanics, pp. 103-117, July 2018

[11] Desai M, Channiwala SA, Nagarsheth HJ. „Experimental and computational aerodynamic investigations of a car”, WSEAS Transactions on Fluid Mechanics, pp. 359-366, October 2008

[12] Cieslinski A. Prym W., Stajuda M., Witkowski D., “Investigation on Aerodynamics of Super–Effective Car for Drag Reduction”, International Journal of Mechanics and Mechanical Engineering, pp. 295-308, September 2016

★★★